Polymer Chemistry

Statistical Copolymers of Thiophene-3-Carboxylates and Selenophene-3-Carboxylates; 77Se NMR as a Tool to Examine Copolymer Sequence in Selenophene-Based Conjugated Polymers

Journal:	*Polymer Chemistry*
Manuscript ID	PY-ART-06-2022-000777.R1
Article Type:	Paper
Date Submitted by the Author:	29-Jul-2022
Complete List of Authors:	Kawakami, Manami; Carnegie Mellon University, Chemistry Schulz, Karl; Carnegie Mellon University, Chemistry Varni, Anthony; Carnegie Mellon University, Chemistry Tormena, Claudio; State University of Campinas, Chemistry Institute Gil, Roberto; Carnegie Mellon University, Chemistry Noonan, Kevin; Carnegie Mellon University, Chemistry

ARTICLE

Statistical Copolymers of Thiophene-3-Carboxylates and Selenophene-3-Carboxylates; ^{77}Se NMR as a Tool to Examine Copolymer Sequence in Selenophene-Based Conjugated Polymers

Received 00th January 20xx,
Accepted 00th January 20xx

DOI: 10.1039/x0xx00000x

Manami Kawakami, [a] Karl Schulz, [a] Anthony J. Varni, [a] Claudio F. Tormena,[b] Roberto R. Gil, [a] and Kevin J.T. Noonan[a] *

Herein, we demonstrate that homopolymerization and statistical copolymerization of 2-ethylhexyl thiophene-3-carboxylate and 2-ethylhexyl selenophene-3-carboxylate monomers is possible via Suzuki-Miyaura cross-coupling. A commercially available palladium catalyst ([1,3-bis(2,6-di-3-pentylphenyl)imidazol-2-ylidene](3-chloropyridyl)dichloropalladium(II) or PEPPSI-IPent) was employed to prepare regioregular conjugated polymers with high molecular weights (~20-30 kg/mol), and relatively narrow molecular weight distributions. The optical bandgap in the copolymer series could be reduced by increasing the concentration of selenophene-3-carboxylate in the material. Configurational triads were observed in the ^{1}H NMR spectra of the statistical copolymers, which were assigned using a combination of 2D NMR techniques. The use of a ^{1}H-^{77}Se HSQC spectrum to further examine sequence distribution in the statistical copolymers revealed how ^{77}Se NMR can be used as a tool to examine the microstructure of Se-containing conjugated polymers.

Introduction

Regioregular poly(3-alkylthiophenes) (*rr*-P3AT),[1] are widely studied organic materials due to the ease of synthesis,[2-6] self-assembly into highly ordered morphologies,[7] good charge mobility,[8] and solution processability. The selenophene analogues, poly(3-alkylselenophenes) (*rr*-P3AS'), have also attracted attention,[9, 10] as they have lower bandgaps and lower redox potentials when compared to *rr*-P3ATs. For these two conjugated polymers, the alkyl side chain is regarded primarily as a solubilizing group, but the choice of side chain in these systems can significantly impact electronic structure, solid-state organization, and processability.

Ester-functionalized polythiophenes such as poly(3-alkylesterthiophenes) (P3AETs – structure shown in Figure 1), have attracted attention since the 1990's[11] as the electron-withdrawing side group enhances the oxidative stability of the polythiophene.[12, 13] An additional benefit of ester groups is straightforward post-polymerization modification via cleavage of the alkyl fragment using bases or heat. Fréchet,[14] Krebs[15, 16] and You[17] have demonstrated that thermal cleavage of ester-functionalized polymers can improve lifetime and stability of organic photovoltaic devices derived from these materials. Reynolds and co-workers have demonstrated that saponification of ester-substituted poly(3,4-propylenedioxythiophenes) can afford insoluble polymers which rapidly and reversibly switch between neutral and oxidized states.[18]

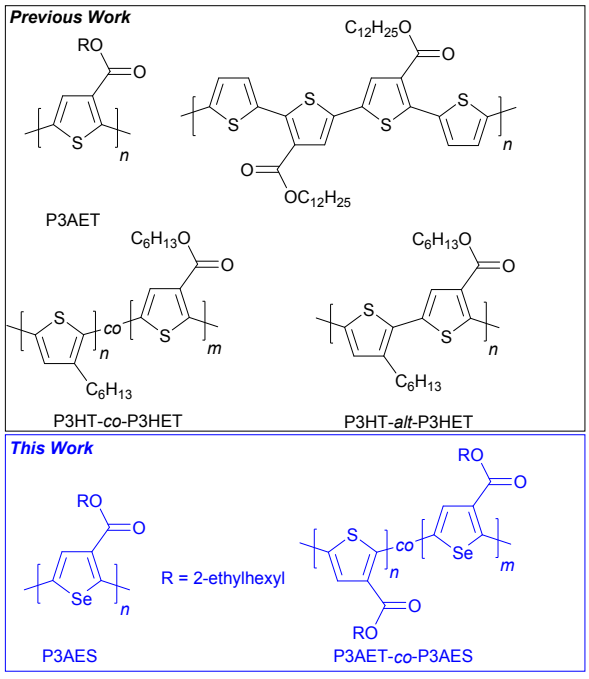

Figure 1. Some examples of ester-functionalized polythiophenes[11-13, 19-21] and the ester-functionalized polyselenophenes synthesized as part of this work.

[a] *Department of Chemistry, Carnegie Mellon University, 4400 Fifth Avenue, Pittsburgh, Pennsylvania 15213, United States*
[b] *Institute of Chemistry, University of Campinas—UNICAMP, P.O. Box 6154, 13083-970 Campinas, Sao Paulo, Brazil*
† Footnotes relating to the title and/or authors should appear here.
Electronic Supplementary Information (ESI) available: [details of any supplementary information available should be included here]. See DOI: 10.1039/x0xx00000x

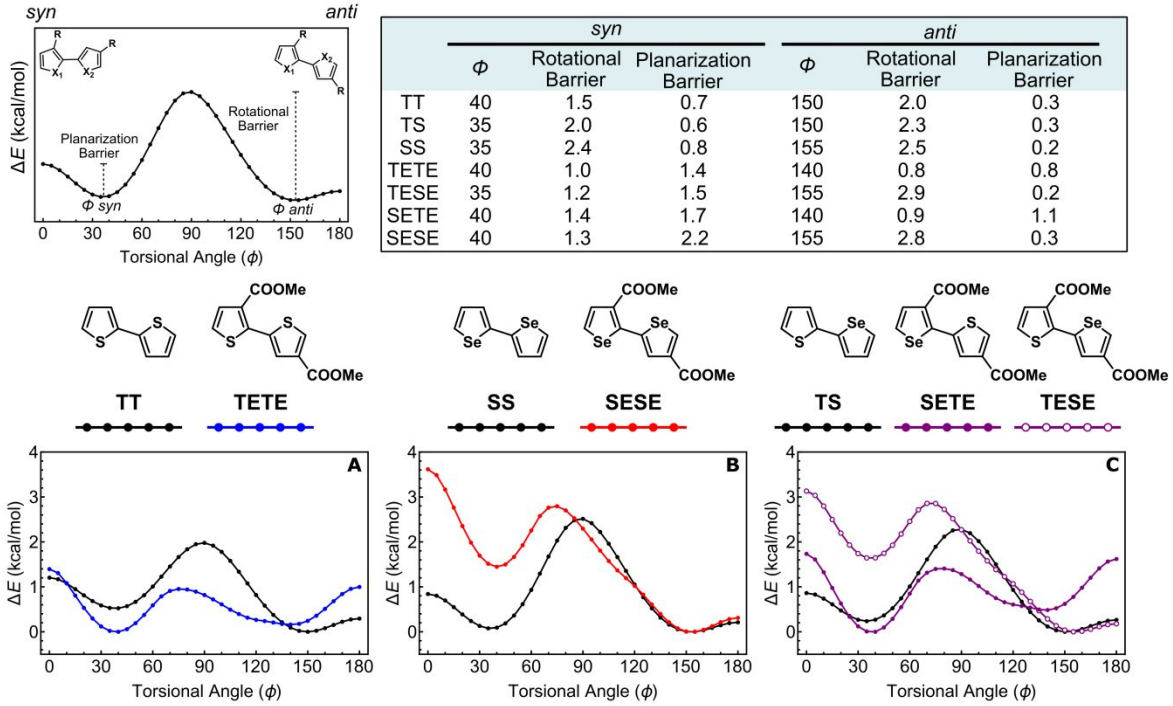

	syn			anti		
	Φ	Rotational Barrier	Planarization Barrier	Φ	Rotational Barrier	Planarization Barrier
TT	40	1.5	0.7	150	2.0	0.3
TS	35	2.0	0.6	150	2.3	0.3
SS	35	2.4	0.8	155	2.5	0.2
TETE	40	1.0	1.4	140	0.8	0.8
TESE	35	1.2	1.5	155	2.9	0.2
SETE	40	1.4	1.7	140	0.9	1.1
SESE	40	1.3	2.2	155	2.8	0.3

Figure 2. Torsional potential energy scans calculated at the ωB97XD/6-31G(d,p) level for various thiophene and selenophene dimers. A) 2,2'-bithiophene (TT, black) and dimethyl [2,2'-bithiophene]-3,4'-dicarboxylate (TETE, blue). B) 2,2'-biselenophene (SS, black), and dimethyl [2,2'-biselenophene]-3,4'-dicarboxylate (SESE, red). C) 2-(selenophen-2-yl)thiophene (TS, black), methyl 5-(3-(methoxycarbonyl)selenophen-2-yl)thiophene-3-carboxylate (SETE, purple, filled) and methyl 2-(4-(methoxycarbonyl)selenophen-2-yl)thiophene-3-carboxylate (TESE, purple, open). The dihedral angles corresponding to local *syn* and *anti* minima, as well as rotational and planarization barriers computed from the torsional scans, are tabulated in the top right.

While the benefits of ester side groups have been well documented,[12-18] achieving high molecular P3AETs is challenging.[11, 20] Moreover, despite the progress in development of ester functionalized polythiophenes, the poly(3-alkylesterselenophenes) (P3AES) analogues have not yet been reported. Ullmann[11, 20] and Kumada[22] coupling were first used to prepare P3AETs, but the polymers were low molecular weight and those prepared using Ullmann coupling were regiorandom. Given the well-known impact of regiodefects in conjugated polymers,[23] methods to build regioregular P3AETs or P3AES' with higher molecular weights are desirable.[22] Thompson has utilized oxidative polymerization and direct arylation to build regioregular P3AETs with M_n values greater than 10 kg/mol (*rr* = 85-99%),[12, 24] and our group developed an approach to construct high molecular weight, regioregular P3AETs using Ni-catalyzed Suzuki-Miyaura cross-coupling (M_n = 20 – 30 kg/mol, *rr* = 98 - 99%).[21]

Here, we demonstrate that high molecular weight, regioregular poly(3-(2-ethylhexyl)esterselenophene (P3(2EH)ES) can be synthesized using Suzuki-Miyaura cross-coupling with a commercially available Pd catalyst (PEPPSI-IPent). In addition, a series of thiophene-3-carboxylate and selenophene-3-carboxylate copolymers were synthesized, where the optical bandgap could be tuned as a function of selenophene content. Controlling the optical properties of random conjugated copolymers has been demonstrated previously,[19, 25-36] but it is particularly important in this case with P3AETs since the absorption spectra of ester-functionalized polythiophenes are typically blue shifted from their alkyl counterparts.[21]

The P3AET-*co*-P3AES copolymers were prepared in good yield with precise control over side chain regioregularity. Relatively complicated signal patterns were observed for the aromatic protons in the ^{1}H NMR spectra of the statistical copolymers, which is due to the different configurational triads that arise from statistical incorporation of the two monomer repeat units along the polymer chain. Using a combination of 2D NMR and computation, the triads could be assigned and suggested smooth incorporation of both monomers in the polymer chain. Moreover, ^{77}Se NMR was used as a tool to resolve the configurational pentads for the polymer, as the Se atoms are highly sensitive to neighbouring monomers in the polymer chain.

Results and Discussion

DFT Calculations. Prior computational work has demonstrated that unsubstituted oligoselenophenes are more rigid than their thiophene counterparts, with higher rotational barriers and shorter inter-ring bonds.[37-41] Here, a series of ester functionalized thiophene (thiophene-3-carboxylate (TE)) and selenophene (selenophene-3-carboxylate (SE)) dimers were investigated and compared to the unsubstituted analogues (Figure 2). More specifically, four ester substituted dimers with identical side chain regiochemistry (TETE, SESE, TESE, and SETE) were examined to gain insight as to the conformational tendencies of the homopolymers and statistical copolymers synthesized herein. Torsional potential energy profiles for all structures were generated by constraining the dihedral angle around the interring bond (defined by X-C-C-X) at 5° intervals

from 0° (*syn*) to 180° (*anti*) and optimizing each conformer (Figure 2, calculations performed at the ωB97XD/6-31G(d,p) level).[40-42]

For all dimers, twisted non-planar forms are preferred with energy minima around 35° – 40° and 140° – 155° (Table in Figure 2). Attachment of the ester group leads to very different outcomes for 2,2'-bithiophene (TT) and 2,2'-biselenophene (SS). A significant 1.2 kcal/mol reduction in the *anti* rotational barrier was noted from TT to TETE (Figure 2A), along with a 0.5 kcal/mol increase in the planarization barrier for the *anti* conformer. Attachment of the ester side groups to the 2,2'-biselenophene clearly destabilizes the *syn* coplanar conformation (2.8 kcal/mol), but the rotational and planarization barriers from the low energy *anti* conformation only increase slightly (Figure 2B). The larger *anti* coplanar planarization barrier (0.8 kcal/mol) for TETE as compared to TT (0.3 kcal/mol), suggests the ester group causes additional steric repulsion in bithiophene. This effect is minimized in the selenophene derivative, with planarization barriers within 0.1 kcal/mol for SS and SESE. In fact, the 0.3 kcal/mol increase in rotational barrier for SESE suggests the ester group will increase the rigidity of polyselenophene.

The computed thiophene-selenophene (TS) dimers also clearly demonstrate the marked impact of the ester group when proximal to thiophene. The parent TSe derivative is like the TT and SS derivatives (Figure 2C, black), with rotational barriers halfway between the two homodimers (Table in Figure 2). When the ester is proximal to the thiophene in SETE, the rotational barrier is reduced and the *anti* planarization barrier is increased just like in TETE (Figure 2C, filled purple circles). The opposite regioisomer with the Se atom proximal to the ester matches closely with SESE (Figure 2C, open purple circles). These results highlight that the proximity of the heavier Se atom to the carbonyl is key to lowering the *anti* planarization barrier, likely due to stronger chalcogen-chalcogen interactions between the oxygen and selenium as compared to the oxygen and sulfur. Altogether, the computational results suggest a lower barrier to *anti* planarization for the poly(3-alkylesterselenophene) homopolymer relative to the poly(3-alkylesterthiophene) homopolymer, as well as a much stronger overall conformational preference (*anti*) for poly(3-alkylesterselenophene). Furthermore, because the SETE and TESE torsional potential energy profiles seem to be predominantly defined by the identity of the heteroatom proximal to the carbonyl, introduction of SE into poly(3-alkylesterthiophenes) should slightly decrease the average energy barrier to *anti* planarization.

Synthesis of P3(2EH)ET and P3(2EH)ES. Suzuki-Miyaura cross-coupling has emerged as a simple method to construct regioregular conjugated polymers with high molecular weights.[43] Choi and co-workers have also demonstrated that the boron group can be used to widen the scope of polymerizable monomers as well as tune reaction kinetics.[44-46] Given the benefits of the Suzuki-Miyaura cross-coupling method, alkyl thiophene-3-carboxylates and alkyl selenophene-3-carboxylates were prepared with bromo and pinacol boronic ester functionalities at the 2 and 5 positions of the heterocyclic ring for use in polymerization (Scheme 1).

The monomers were prepared in a three-step sequence, starting from the thiophene or selenophene-3-carboxylic acid. Bromination at the 2-position is accomplished by *ortho*-directed metalation with *n*-butyllithium (*n*BuLi), followed by electrophilic quenching with Br_2 (64% for T and 79% for S). Esterification is then accomplished in dimethylformamide with an alkyl halide and K_2CO_3. It should be noted that hexyl or 2-ethylhexyl side chains can be installed using this approach, however, the poly(3-hexylesterselenophene) (P3HES) has limited solubility, so the bulk of this work was focused on branched side chains to afford THF soluble polymers for straightforward molecular weight analysis.

The pinacol boronic ester can be installed at the 5-position of the heterocycle using iridium-catalyzed borylation,[47] or by metalation[12] and electrophilic quenching with a borate (Methods A and B, respectively in Scheme 1). The iridium-catalysed C-H borylation was highly effective for synthesis of the thiophene derivative (3(2EH)ET).[21] Unfortunately, the iridium-catalysed reaction was less effective for the selenophene, and the precise reason for this difference between the thiophene and selenophene borylation is unclear. Consequently, the 3(2EH)ES monomer was synthesized using Method B, where 2-bromoselenophene-3-carboxylate was metalated at the 5-position using 2,2,6,6-tetramethylpiperidinylmagnesium chloride lithium chloride complex solution (TMPMgCl·LiCl), and quenched with 2-isopropoxy-4,4,5,5-tetramethyl-1,3,2-dioxaborolane (*i*PrO-Bpin). The 3(2EH)ES monomer was obtained in 76% yield using this approach.

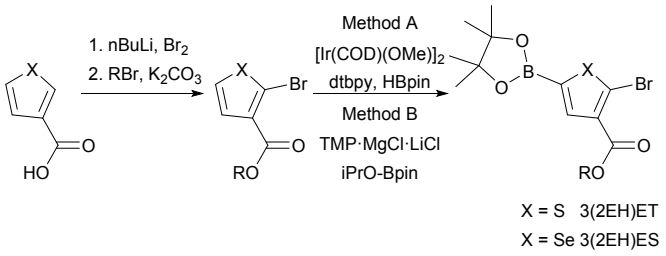

Scheme 1. General synthetic approach to the ester-functionalized monomers. The abbreviations are as follows: *n*BuLi – n-butyllithium, $[Ir(COD)(OMe)]_2$ - (1,5-cyclooctadiene)(methoxy)iridium(I) dimer, dtbpy - 4,4′-di-*tert*-butyl-2,2′-dipyridyl, HBpin – pinacolborane, TMP·MgCl·LiCl - 2,2,6,6-tetramethylpiperidinylmagnesium chloride lithium chloride complex solution, iPrO-Bpin - 2-isopropoxy-4,4,5,5-tetramethyl-1,3,2-dioxaborolane.

We envisioned using $Ni(IPr)(PPh_3)Cl_2$ for polymerization of 3(2EH)ET and 3(2EH)ES similar to prior work,[21] but unfortunately, we encountered issues with the commercially supplied catalyst. Specifically, the ^1H NMR spectrum for $Ni(IPr)(PPh_3)Cl_2$ (TCI, Lot # FJLZN-GK), was markedly different than expected (Figure S11), suggesting reproducibility issues may arise. Since commercial catalysts are highly desirable, we explored other alternatives for the preparation of P3(2EH)ET and P3(2EH)ES.

Table 1. Optimization of polymerization conditions for the preparation of P3(2EH)ET and P3(2EH)ES

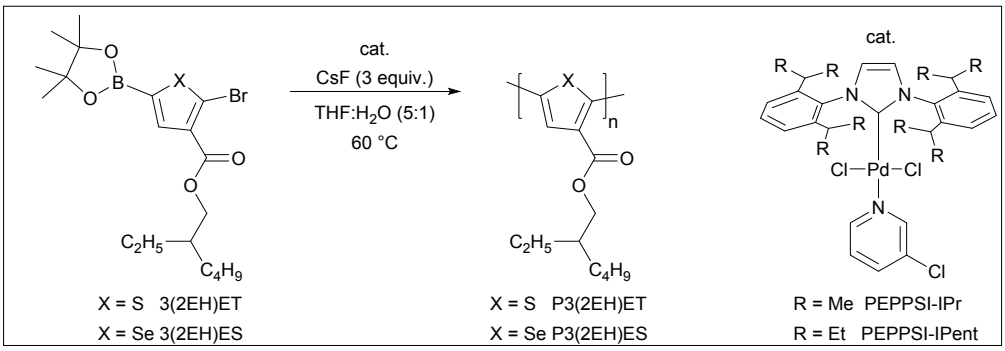

Entry[a]	X	Catalyst (equiv)	Additive (equiv)	Conc. (mM)	Time (min)	M_n (kg/mol)[b]	$Đ$[b]	Yield (%)
1	S	PEPPSI-IPr (3 mol %)	None	30	240	11.6	1.17	>99
2	S	PEPPSI-IPent (3 mol %)	None	30	60	28.4	1.11	>99
3	S	PEPPSI-IPent (3 mol %)	PPh_3 (3 mol %)	30	180	31.0	1.29	>99
4	S	PEPPSI-IPent (5 mol %)	PPh_3 (5 mol %)	30	180	28.9	1.15	81
5	Se	PEPPSI-IPent (3 mol %)	PPh_3 (3 mol %)	15	180	27.1[c]	1.35	88
6	Se	PEPPSI-IPent (5 mol %)	PPh_3 (5 mol %)	15	180	27.3[c]	1.38	76

[a]All reactions were conducted at 60 °C. Typical polymerization conditions were as follows: 0.12 mmol of monomer, 0.36 mmol of CsF, 5:1 = THF:H_2O. Polymerizations were quenched with 6M HCl/MeOH. [b]GPC traces were recorded versus polystyrene standards at 40 °C with THF as the eluent.[c] The P3(2EH)ES polymers aggregate upon standing in THF with and precipitation over time.

We considered whether another metal N-heterocyclic carbene (NHC) catalyst could be used in place of the nickel. PEPPSI catalysts are commercially available and have been employed previously in polythiophene synthesis.[48-52] Both Pd-PEPPSI-IPr and Pd-PEPPSI-IPent (structures shown in Table 1)[53] were examined for polymerization of 3(2EH)ET (Table 1, entries 1-2). We noted that high molecular weight P3(2EH)ET was formed faster using the PEPPSI-IPent catalyst, so it was employed as the catalyst for all subsequent polymerizations.

Polymerization of 3(2EH)ET (30 mM) was carried out at 60 °C in 5:1 THF:H_2O, with 3 equivalents of CsF as the inorganic base. After 1 h, the polymer was precipitated from the reaction solution with 6 M HCl/MeOH. Under these conditions, P3(2EH)ET was obtained in high yield with an M_n =28.4 kg/mol (Table 1, entry 2). It should be noted that for all synthesized polymers, molecular weight analysis using gel permeation chromatography (GPC) was carried out on samples washed only with MeOH. However, to ensure ^{1}H NMR spectra of polymers were free from minor impurities, samples were washed with copious amounts of hot acetone.

In prior work, reductive elimination of NHCs with arenes to yield polymers with imidazolium end groups has been noted as a possible side reaction in cross-coupling polymerization.[54] This is also well known in stoichiometric investigations of (NHC)M(R)X compounds.[55-57] In an effort to limit this side reaction, an equivalent of triphenylphosphine (PPh_3) was added for polymerizations of 3(2EH)ET and 3(2EH)ES (Table 1, entries 3-6). Grushin and coworkers have noted in studies on IPrPd(Ph)Cl that PPh_3 can help suppress reductive elimination of IPr-Ph.[55] Though polymerizations were markedly slower upon inclusion of the additional PPh_3, M_n values of the final polymers were still between 25 – 30 kg/mol (Table 1, entries 3-6). Reaction conditions employed for the polymerization of 3(2EH)ES were similar to 3(2EH)ET, except the monomer concentration was cut in half to 15 mM to prevent aggregation and premature precipitation of the polymer during the reaction. The molecular weight distributions for the P3(2EH)ES polymers were wider than those for P3(2EH)ET (Table 1, entries 5-6), with M_n values around 27 kg/mol for P3(2EH)ES. The fairly narrow molecular weight distributions noted for both P3(2EH)ET and P3(2EH)ES ($Đ$ = 1.1 – 1.4) suggested perhaps a chain-growth mechanism was operative, but changes in catalyst loading did not result in the expected change in M_n.

NMR spectroscopy. The newly synthesized P3(2EH)ES is regioregular, as evidenced by the aromatic region of the ^{1}H NMR spectrum for the polymer sample (Figure 3, bottom). A major signal is observed at 8.08 ppm, corresponding to the aromatic C-H proton of the selenophene ring within the polymer main chain (H^A). This signal is shifted downfield as compared to the thiophene homopolymer (P3(2EH)ET at 7.83 ppm, H^A in Figure 3). COSY spectra were used to assign several minor signals observed in each of the spectra, which correspond to end group signals and minor defects from catalyst initiation.[58] The minor signals observed in the ^{1}H NMR spectrum for P3(2EH)ES are very similar to the thiophene analog, which has been assigned previously.[21] PEPPSI-IPent is a metal dihalide, so this results in a tail-to-tail (TT) defect from precatalyst reduction. This TT signal appears at 7.68 ppm (H^B) for P3(2EH)ES, relatively close to the TT signal observed for P3(2EH)ET at 7.58 ppm. The aromatic proton for the Br-terminated end group in P3(2EH)ES appears at 7.95 ppm (H^C), again downfield from the same signal in P3(2EH)ET (7.66 ppm). The aromatic proton of the ring next to the Br-terminated end group was also assigned using 2D NMR spectroscopy (7.79 ppm for P3(2EH)ET and 8.04 ppm for P3(2EH)ES). Since the polymerization was quenched with 6 M HCl/MeOH, if the

reaction proceeded by a chain-growth mechanism, a 1:1 ratio of H and Br chain ends would be expected (1:1:1 ratio of H_C:H_D:H_E). In all cases, the concentration of Br end groups (H_C) was larger than the concentration of H end groups (H_D:H_E), suggesting a more complicated mechanism.

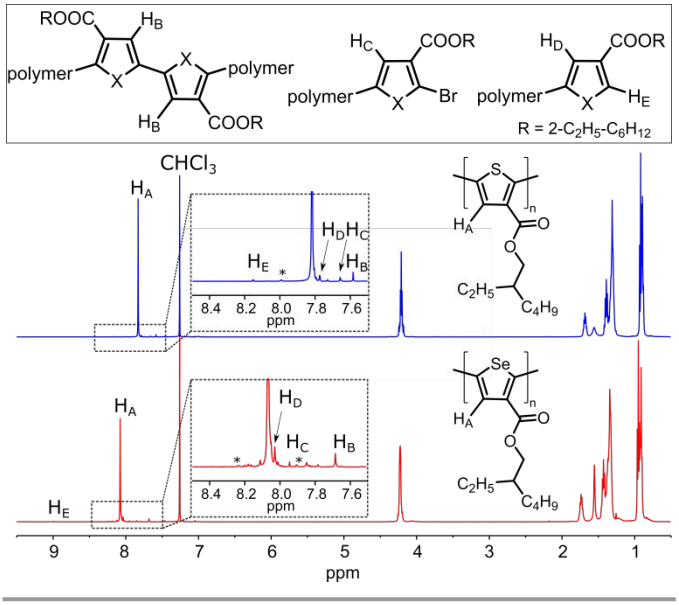

Figure 3. ^{1}H NMR spectra (500 MHz, 25 °C) of P3(2EH)ET (top, M_n = 31.0 kg/mol), and P3(2EH)ES (bottom, M_n = 26.5 kg/mol) collected in $CDCl_3$. The ^{13}C satellite signals are denoted with a * in the inset.

The degree of polymerization (DP_n) for P3(2EH)ET or P3(2EH)ES synthesized with PEPPSI-IPent was much higher than expected based on catalyst loading. When targeting DP_n = 33 for P3(2EH)ET (Table 1, entry 2), the DP_n determined from comparison to the TT defect was more than double the expected value (DP_n = 94, Figure S18). This suggests a portion of the catalyst added to the reaction is inactive in polymerization.[21] Ananikov and coworkers have demonstrated that metal carbene complexes can hydrolyze under basic conditions,[59, 60] suggesting a portion of the precatalyst could be hydrolyzed at the outset of the reaction. We have also noted that 1,3-bis(diphenylphosphino)propanedichloronickel(II) precatalysts partially hydrolyze in Suzuki-Miyaura polymerization.[61]

Synthesis of P3(2EH)ET-*co*-P3(2EH)ES. Since both thiophene and selenophene-3-carboxylates were polymerized effectively using PEPPSI-IPent, copolymerizations were also examined. The statistical copolymers are designated as ***stat*-TSe$_{Xi}$** where X_i corresponds to targeted mol % selenophene (Table 2). Polymerizations with varying ratios of the two monomers (Se_{Xi} = 33, 50 67%) using PEPPSI-IPent afforded copolymers in high yields (77 – 83%), with M_n's above 30 kg/mol (Table 2). The mole fraction of Se incorporated into the polymer was slightly lower than the target as determined by ^{1}H NMR spectroscopy, but within 5% in all cases (Table 2).

Table 2. Copolymerizations of 3(2EH)ET and 3(2EH)ES using PEPPSI-IPent.

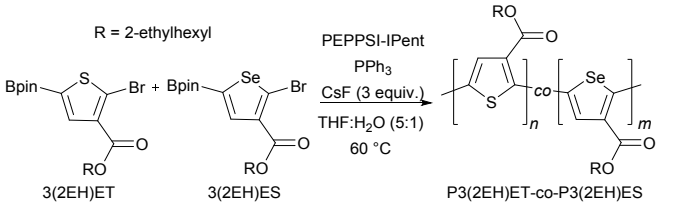

Entry	Targeted T:Se ratio (mol:mol)	% Se in Polymer (^{1}H NMR)	M_n (kg/mol)	$Đ$	Yield (%)
stat-TSe$_{33}$	2:1	29	33.8	1.10	77
stat-TSe$_{50}$	1:1	47	33.4	1.15	83
stat-TSe$_{67}$	1:2	63	30.3	1.16	77

At a glance, the aromatic region in the 500 MHz 1D ^{1}H NMR spectrum in $CDCl_3$ of the *stat*-TSe copolymers are markedly more complicated than the ^{1}H NMR spectra of poly(3-hexylthiophene)-*co*-poly(3-hexylselenophene) statistical copolymers.[36] The large number of signals noted in the *stat*-TSe spectra here suggests improved spectral resolution, likely due to the presence of the electron-withdrawing ester substituents. This is similar to regioirregular P3HET, where pentads were observed in the aromatic region.[20]

Two distinct groups of aromatic proton signals appear in the chemical shift ranges of 8.3 – 8.0 ppm and 7.9 – 7.7 ppm (Figure 4). Each chemical shift region shows four well resolved signals which were attributed to the 4 thiophene-centered triads (T***T***T, Se***T***T, T***T***Se, Se***T***Se) and the 4-selenophene centered triads (Se***Se***Se, T***Se***Se, Se***Se***T, TSeT). The signals at 7.83, 7.80, 7.77, 7.73 ppm correspond to the thiophene-centered trials while those at 8.17, 8.14, 8.12, 8.08 correspond to the selenophene-centered trials (Figure 4). The P3(2EH)ET and P3(2EH)ES homopolymers enable assignment of 7.83 and 8.08 as the T***T***T and Se***Se***Se triads, respectively (Figure 4).

We considered ^{77}Se NMR spectroscopy as a tool to offer additional insight into the triad assignments given the exceptionally large chemical shift range for ^{77}Se, and the sensitivity of Se atoms to the local environment in organic molecules. Indeed, a ^{1}H-^{77}Se HSQC spectrum revealed the expected 16 signals for all the Se centered pentads (Figure 5, Top). Moreover, the Se atoms are clearly highly sensitive to the environment, as the two major signals are separated by nearly 12 ppm. Additionally, the chemical shift of the Se atom at the center of the triads strongly depends on the nature of the subunit attached to the left while the subunit attached to the right has a much smaller effect (12 ppm vs <1 ppm, respectively). Using this 2D spectrum, and computed shielding constants for the triads (Supporting Information), it was possible to assign the Se-centered triads 8.17 (T***Se***T), 8.14 (Se***Se***T), 8.12 (T***Se***Se), 8.08 (Se***Se***Se).

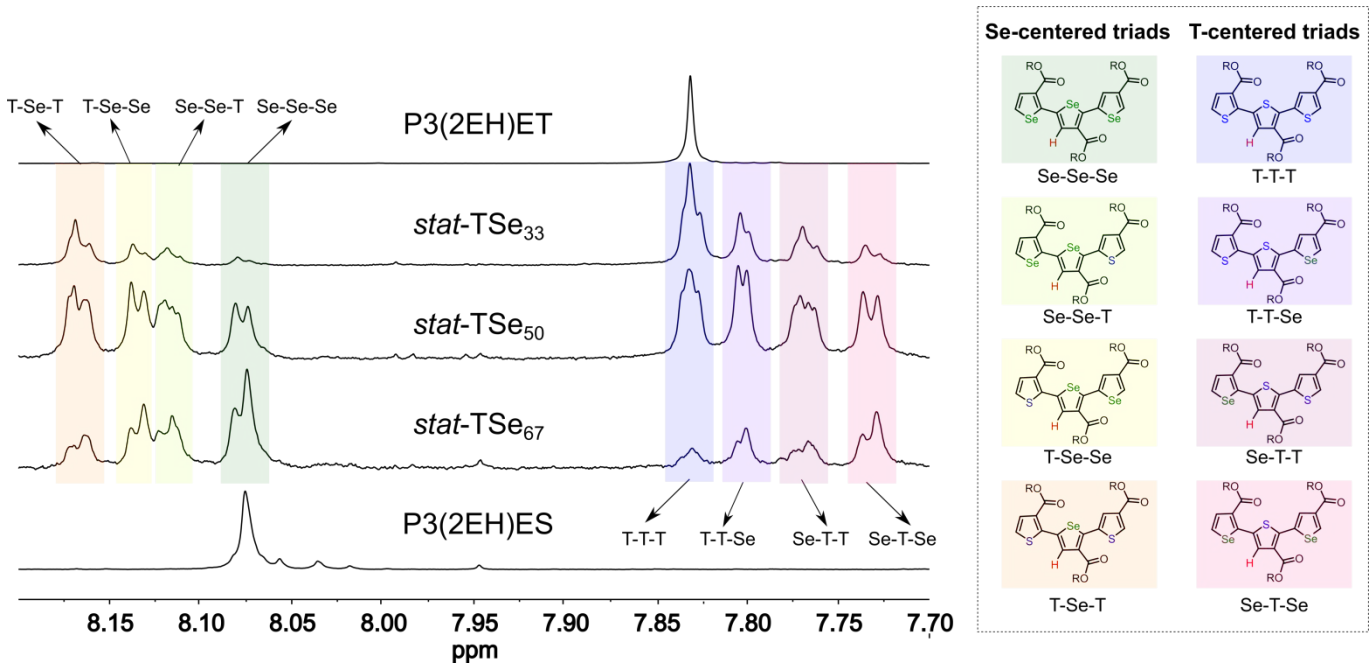

Figure 4. Left - Stacked ^{1}H-NMR spectra of P3(2EH)ET (M_n = 38.4 kg/mol), *stat*-TSe$_{33}$ (M_n = 33.8 kg/mol), *stat*-TSe$_{50}$ (M_n = 33.4 kg/mol), *stat*-TSe$_{67}$ (M_n = 30.3 kg/mol), and P3(2EH)ES (M_n = 31.8 kg/mol). Right – Eight possible configurational triads for the copolymers.

The T-centered triads could also be assigned again with the aid of computed shielding constants: 7.83 (T***T***T), 7.80 (T***T***Se), 7.77 (Se***T***T), 7.73 (Se***T***Se) ppm. The ^{1}H-^{13}C HMBC spectrum also allowed for the assignment of the carbon atoms at the point of contact between subunits via common correlations between thiophene and selenophene protons (Figure 5, Bottom).

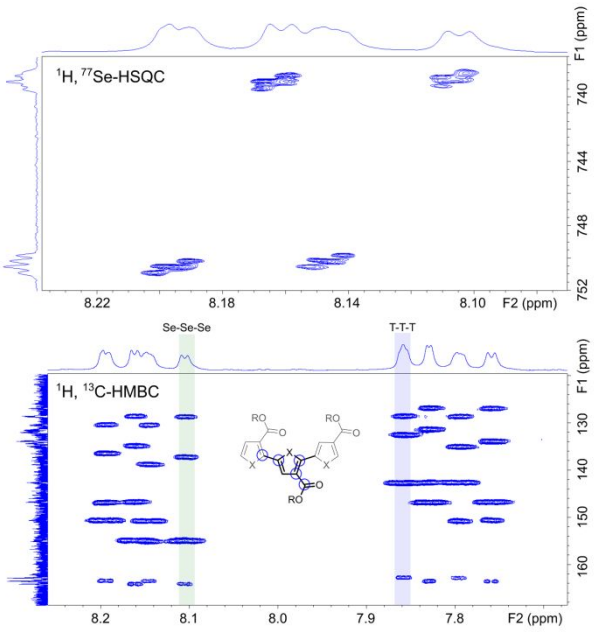

Figure 5. (Top) ^{1}H-^{77}Se HSQC spectrum of *stat*-TSe$_{50}$ with 16 signals for all the Se centered pentads. (Bottom) ^{1}H-^{13}C HMBC spectrum of *stat*-TSe$_{50}$ illustrating the 4 expected correlations for Se***Se***Se and T***T***T triad.

Both the $J_{H,Se}$-optimized HSQC and ^{1}H-^{13}C HMBC correlation experiments clearly show that each triad signal splits into four well-resolved cross-correlation peaks, attributed to four pentads per triad, which are not all well resolved in the 1D ^{1}H NMR spectrum (Figure 5). Hence, the combination of 1D and 2D NMR experiments allows the clear observation of the 32 pentads for the *stat*-TSe$_{50}$ copolymer.

Finally, the NMR spectra enable estimation of reactivity ratios for the copolymerization. Copolymer reactivity ratios are often determined by examining instantaneous copolymer composition at low conversion (~5%) in polymerization reactions (Mayo-Lewis model). This type of analysis would be difficult in the current study, as gas chromatography with these monomers is challenging (Figure S33), and distinguishing between monomer and polymer is difficult in crude ^{1}H NMR spectra. Fortunately, the average copolymer composition is coded into the polymer by the relative ratios of the different triads. Assuming a terminal copolymer model, the sequence distributions and the starting feed ratios can be used to provide rough estimates of the thiophene reactivity ratio (r_T) using the equation below.[62] The Se triad data can be used to obtain the r_{Se} in an analogous manner.

$$\frac{N_{TTT} + N_{TTSe} + N_{SeTT} + N_{SeTSe}}{N_{SeTSe} + \frac{N_{TTSe} + N_{SeTT}}{2}} = r_T \frac{[3(2EH)ET]}{[3(2EH)ES]} + 1$$

Using this equation, and the integration data for the triads of the final polymers as obtained from the ^{1}H NMR spectra shown in Figure 5, the reactivity ratios can be estimated (r_T = 1.16 ± 0.05 and r_{Se} = 0.83 ± 0.03). These values indicate a near random copolymerization. Altogether, the 1D and 2D NMR data provide a wealth of information on regioregularity and end group signals, degree of polymerization, chain microstructure and monomer reactivity.

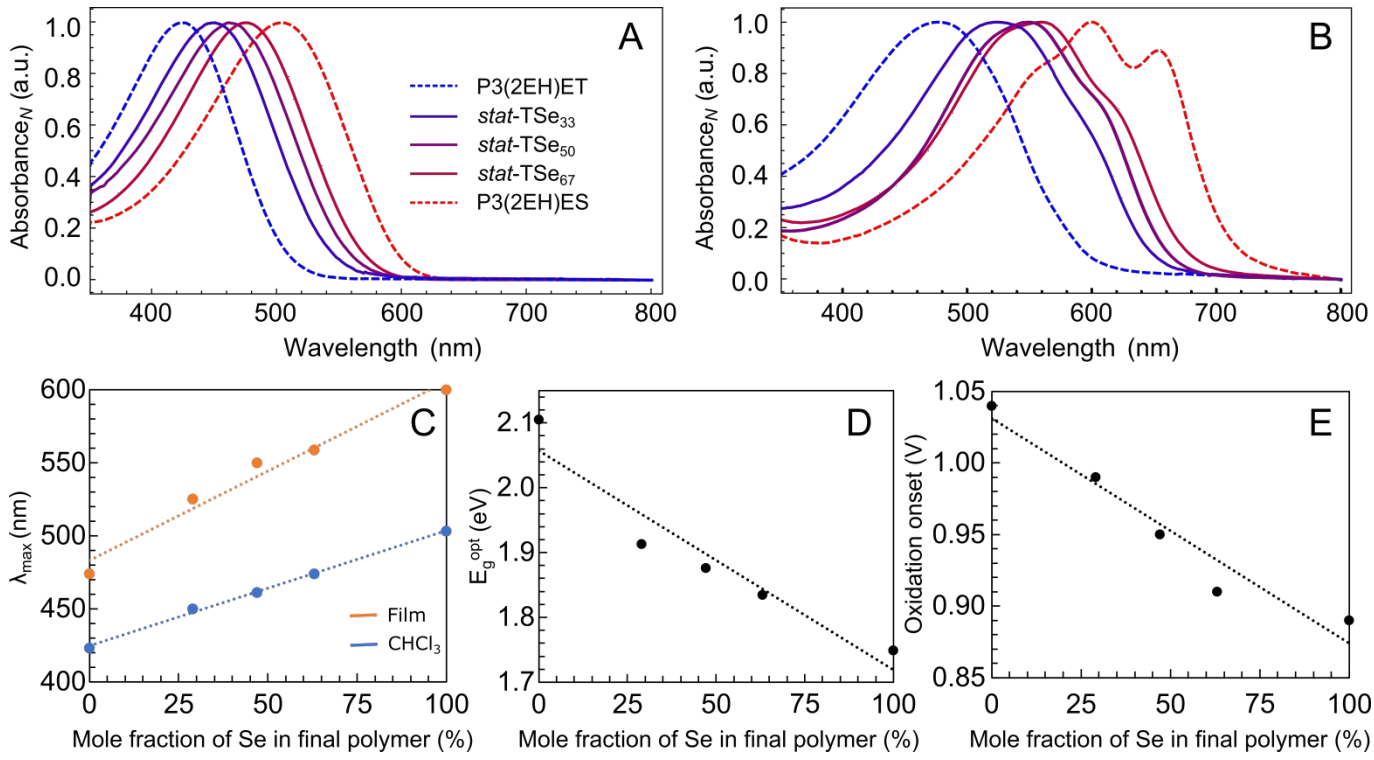

Figure 6. A) Solution UV-vis spectra collected in $CHCl_3$ at 0.0075 mg/mL concentrations and B) Solid-state UV-vis spectra for P3(2EH)ET (dashed blue, M_n = 38.4 kg/mol), *stat*-TSe_{33} (solid blue, M_n = 33.8 kg/mol), *stat*-TSe_{50} (solid purple, M_n = 33.4 kg/mol), *stat*-TSe_{67} (solid red, M_n = 30.3 kg/mol), and P3(2EH)ES (dashed red, M_n = 31.8 kg/mol). C) Mole fraction of selenophene in the final polymer versus λ_{max} (nm) in film (orange) and solution (blue). D) Mole fraction of selenophene in the final polymer versus optical bandgaps calculated from solid-state absorption spectra (ν_{edge}, eV). E) Mole fraction of selenophene in the final polymer versus oxidation onset estimated form cyclic voltammetry studies. Cyclic voltammograms were collected on solid films by drop-casting the sample onto the working electrode from a 5 mg/mL solution in $CHCl_3$, and scanning across a potential range in acetonitrile [0.40 V ($E_{Fc/Fc+}$) vs. SCE for MeCN] with tetrabutylammonium hexafluorophosphate as the supporting electrolyte (0.1 M). Voltammograms were recorded at a scan rate of 100 mV/s with a glassy carbon working electrode.

Optical Properties and Oxidation Potentials of Synthesized Polymers. The HOMO levels of the homopolymers and statistical copolymers was probed using cyclic voltammetry (CV) (Figure S22 - S26). Optical bandgaps were also calculated from the absorption edge (ν_{edge}) using UV-vis spectroscopy (Figure S27 – S31). These two techniques provide a clear picture of the impact of the Se ring in these polymeric systems (Figure 6). It is clear that the bandgap decreases with increasing Se content in the polymer chain, consistent with prior observations on statistical copolymers of poly(3-hexylthiophene) and poly(3-hexylselenophene) (P3HT-*co*-P3HS).[36] Solution and solid-state spectra both exhibited a red-shift in absorbance maxima with increasing concentration of Se (Figure 6A and 6B). A linear correlation was observed between the absorbance maxima and the selenophene content (Figure 6C). The λ_{max} values span nearly 80 nm in solution (423 nm to 503 nm) and 130 nm in solid-state (474 nm to 600 nm), while the ν_{edge} in the solid state spans 120 nm (589 to 709 nm) moving from P3(2EH)ET to P3(2EH)ES. The optical bandgap for the copolymers decreases with increasing Se content, as expected (Figure 6D), though it is not a perfectly linear trend. The bandgap for P3(2EH)ES (1.75 eV) is slightly higher than related selenophene polymers such as P3HS (1.6 eV)[9] and poly(3-tridecylketoselenophene) (1.5 eV).[63] Part of the blue shift in this ester polymer may be attributed to the branched side chain.

The quasi-reversible oxidation potential onsets for the statistical copolymers decreased slightly with increasing concentration of the Se ring, from 1.04 V for P3(2EH)ET to 0.89 eV for P3(2EH)ES (Figure 6E). Examination of the solid-state absorption spectra revealed differences between the vibronic structure for P3(2EH)ET, P3(2EH)ES, and the statistical copolymers (Figure 6B), even though all polymers were drop-cast identically from $CHCl_3$ and annealed at 150 °C for 40 min. The $A_{0\text{-}0}$ vibronic peak is notably absent in the solid-state absorption spectrum for P3(2EH)ET (Figure 6B, red), it is present but weak in the statistical copolymers, and it is well defined and distinguishable for P3(2EH)ES (Figure 6B, blue). This suggests improved ordering in the solid-state according to the model developed by Spano and co-workers to describe photophysical behaviour of P3HT.[64, 65] In that work, they note that the ratio of the $A_{0\text{-}0}$ and $A_{0\text{-}1}$ peaks in the absorption spectrum relate to the free-exciton bandwidth and the vibrational energy of the C=C symmetric stretch of the ring.[64, 65] The value of the exciton bandwidth can then be used to quantify the degree of excitonic coupling within polymer aggregates which is related to intra-chain order including average conjugation length and crystallinity.[64, 65] The absence of the $A_{0\text{-}0}$ signal in P3(2EH)ET and

the appearance of it in the statistical copolymers and P3(2EH)ES, suggests the Se-3-carboxylate is beneficial for improved intra-chain ordering in the solid-state, as anticipated from the computer dimers.

Conclusions

In conclusion, we have synthesized a new class of ester functionalized polychalcogenophene, specifically the poly(3-alkylesterselenophene). In addition, we have synthesized a series of poly(3-alkylesterthiophene)-*co*-poly(alkylesterselenophene) copolymers. The commercially available PEPPSI-IPent catalyst enabled the synthesis of all these regioregular polymers with high molecular weights (M_n ~30 kg/mol), and relatively narrow molecular weight distributions. The large number of signals noted in the ^{1}H NMR spectra of the statistical copolymers was attributed to the configurational triads arising from the statistical incorporation of the two repeat units. A 2D HSQC ^{1}H-^{77}Se spectrum also revealed the exceptional sensitivity of the Se atom to local environment in these polymers, suggesting this technique would be beneficial for examining polymer microstructure, end groups or defects of other Se containing conjugated polymers.

The optical properties of the statistical copolymers were dependent on the concentration of selenophene in the polymer, and a near linear correlation was noted for absorbance maxima plotted against Se concentration. The absence of the vibronic structure in P3(2EH)ET and the appearance of it in the statistical copolymers and P3(2EH)ES, suggests the selenophene-3-carboxylate along the polymer backbone is beneficial for improved intra-chain ordering in the solid-state. Future work will focus on more extensive characterization of these materials in in the solid-state using X-ray scattering, differential scanning calorimetry, and atomic force microscopy. Key to this will be exploration of linear and branched side chains, to better understand the role of the side chain in solid-state organization.

Conflicts of interest

There are no conflicts to declare

Acknowledgements

KJTN is grateful to the NSF for support of this work (CHE-2109065). CFT is grateful to the Sao Paulo Research Foundation (FAPESP) for providing financial support for this research, through grant #2020/10246-0 and for Brazilian Research Council (CNPq) for fellowship. All authors are grateful to Prof. Gary E. Martin from Seton Hall University for helpful suggestions regarding the application of ^{77}Se NMR to our structural problem, and Clemens Anklin from Bruker BioSpin Corporation for helping us to choose the most appropriate Bruker pulse program to run ^{1}H,^{77}Se correlation experiments.

References

1. I. F. Perepichka and D. F. Perepichka, eds., *Handbook of Thiophene-based Materials: Applications in Organic Electronics and Photonics*, John Wiley & Sons, Ltd, Chichester, UK, 2009.
2. M. C. Iovu, E. E. Sheina, R. R. Gil and R. D. McCullough, *Macromolecules*, 2005, **38**, 8649-8656.
3. E. E. Sheina, J. Liu, M. C. Iovu, D. W. Laird and R. D. McCullough, *Macromolecules*, 2004, **37**, 3526-3528.
4. R. D. McCullough and R. D. Lowe, *J Chem. Soc. Chem. Commun.*, 1992, 70-72.
5. A. Yokoyama, R. Miyakoshi and T. Yokozawa, *Macromolecules*, 2004, **37**, 1169-1171.
6. R. Miyakoshi, A. Yokoyama and T. Yokozawa, *Macromol. Rapid Commun.*, 2004, **25**, 1663-1666.
7. R. Zhang, B. Li, M. C. Iovu, M. Jeffries-EL, G. Sauvé, J. Cooper, S. Jia, S. Tristram-Nagle, D. M. Smilgies, D. N. Lambeth, R. D. McCullough and T. Kowalewski, *J. Am. Chem. Soc.*, 2006, **128**, 3480-3481.
8. J.-F. Chang, B. Sun, D. W. Breiby, M. M. Nielsen, T. I. Sölling, M. Giles, I. McCulloch and H. Sirringhaus, *Chem. Mater.*, 2004, **16**, 4772-4776.
9. M. Heeney, W. Zhang, D. J. Crouch, M. L. Chabinyc, S. Gordeyev, R. Hamilton, S. J. Higgins, I. McCulloch, P. J. Skabara, D. Sparrowe and S. Tierney, *Chem. Commun.*, 2007, 5061-5063.
10. J. Hollinger, A. A. Jahnke, N. Coombs and D. S. Seferos, *J. Am. Chem. Soc.*, 2010, **132**, 8546-8547.
11. M. Pomerantz, H. Yang and Y. Cheng, *Macromolecules*, 1995, **28**, 5706-5708.
12. N. S. Gobalasingham, S. Noh and B. C. Thompson, *Polym. Chem.*, 2016, **7**, 1623-1631.
13. A. R. Murphy, J. Liu, C. Luscombe, D. Kavulak, J. M. J. Fréchet, R. J. Kline and M. D. McGehee, *Chem. Mater.*, 2005, **17**, 4892-4899.
14. J. Liu, E. N. Kadnikova, Y. Liu, M. D. McGehee and J. M. J. Fréchet, *J. Am. Chem. Soc.*, 2004, **126**, 9486-9487.
15. M. Manceau, E. Bundgaard, J. E. Carlé, O. Hagemann, M. Helgesen, R. Søndergaard, M. Jørgensen and F. C. Krebs, *J. Mater. Chem.*, 2011, **21**, 4132-4141.
16. M. Manceau, M. Helgesen and F. C. Krebs, *Polym. Degrad. Stab.*, 2010, **95**, 2666-2669.
17. S. Y. Son, S. Samson, S. Siddika, B. T. O'Connor and W. You, *Chem. Mater.*, 2021, **33**, 4745-4756.
18. B. D. Reeves, E. Unur, N. Ananthakrishnan and J. R. Reynolds, *Macromolecules*, 2007, **40**, 5344-5352.
19. S. Noh, N. S. Gobalasingham and B. C. Thompson, *Macromolecules*, 2016, **49**, 6835-6845.
20. M. Pomerantz, Y. Cheng, R. K. Kasim and R. L. Elsenbaumer, *Synth. Met.*, 1997, **85**, 1235-1236.
21. Y. Qiu, J. C. Worch, A. Fortney, C. Gayathri, R. R. Gil and K. J. T. Noonan, *Macromolecules*, 2016, **49**, 4757-4762.
22. A. S. Amarasekara and M. Pomerantz, *Synthesis*, 2003, 2255-2258.
23. Y. Kim, H. Park, J. S. Park, J.-W. Lee, F. S. Kim, H. J. Kim and B. J. Kim, *J. Mater. Chem. A*, 2022, **10**, 2672-2696.
24. R. M. Pankow, L. W. Ye and B. C. Thompson, *Macromolecules*, 2020, **53**, 3315-3324.
25. J. B. Howard and B. C. Thompson, *Macromol. Chem. Phys.*, 2017, **218**, 1700255.

26. B. Xu, S. Noh and B. C. Thompson, *Macromolecules*, 2014, **47**, 5029-5039.
27. B. Burkhart, P. P. Khlyabich and B. C. Thompson, *Macromolecules*, 2012, **45**, 3740-3748.
28. H. Yan, J. Hollinger, C. R. Bridges, G. R. McKeown, T. Al-Faouri and D. S. Seferos, *Chem. Mater.*, 2014, **26**, 4605-4611.
29. L. M. Kozycz, D. Gao and D. S. Seferos, *Macromolecules*, 2013, **46**, 613-621.
30. J. H. Bannock, M. Al-Hashimi, S. H. Krishnadasan, J. J. M. Halls, M. Heeney and J. C. de Mello, *Mater. Horizons*, 2014, **1**, 214-218.
31. E. F. Palermo and A. J. McNeil, *Macromolecules*, 2012, **45**, 5948-5955.
32. M. J. Minkler, J. Kim, K. E. Lawson, A. Ali, R. Zhao, A. J. Adamczyk and B. S. Beckingham, *Mater. Lett.*, 2019, **256**, 126563.
33. M. J. Minkler and B. S. Beckingham, *Mater. Today Commun.*, 2019, **20**, 100547.
34. T. Hardeman and G. Koeckelberghs, *Macromolecules*, 2015, **48**, 6987-6993.
35. T. Hardeman and G. Koeckelberghs, *Macromolecules*, 2014, **47**, 8618-8624.
36. A. Fortney, C.-H. Tsai, M. Banerjee, D. Yaron, T. Kowalewski and K. J. T. Noonan, *Macromolecules*, 2018, **51**, 9494-9501.
37. S. S. Zade, N. Zamoshchik and M. Bendikov, *Chem. Eur. J.*, 2009, **15**, 8613-8624.
38. S. S. Zade and M. Bendikov, *Chem. Eur. J.*, 2007, **13**, 3688-3700.
39. V. Topolskaia, A. A. Pollit, S. Cheng and D. S. Seferos, *Chem. Eur. J.*, 2021, **27**, 9038-9043.
40. J. B. Lin, Y. Jin, S. A. Lopez, N. Druckerman, S. E. Wheeler and K. N. Houk, *J. Chem. Theory and Comput.*, 2017, **13**, 5624-5638.
41. J. W. G. Bloom and S. E. Wheeler, *J. Chem. Theory and Comput.*, 2014, **10**, 3647-3655.
42. S. Samdal, E. J. Samuelsen and H. V. Volden, *Synth. Met.*, 1993, **59**, 259-265.
43. M. V. Bautista, A. J. Varni, J. Ayuso-Carrillo, M. C. Carson and K. J. T. Noonan, *Polym. Chem.*, 2021, **12**, 1404-1414.
44. H. Park, J. Lee, S.-H. Hwang, D. Kim, S. H. Hong and T.-L. Choi, *Macromolecules*, 2022, **55**, 3476-3483.
45. J. Lee, H. Kim, H. Park, T. Kim, S.-H. Hwang, D. Seo, T. D. Chung and T.-L. Choi, *J. Am. Chem. Soc.*, 2021, **143**, 11180-11190.
46. J. Lee, H. Park, S.-H. Hwang, I.-H. Lee and T.-L. Choi, *Macromolecules*, 2020, **53**, 3306-3314.
47. G. A. Chotana, V. A. Kallepalli, R. E. Maleczka Jr. and M. R. Smith III, *Tetrahedron*, 2008, **64**, 6103-6114.
48. K. Mikami, M. Nojima, Y. Masumoto, Y. Mizukoshi, R. Takita, T. Yokozawa and M. Uchiyama, *Polym. Chem.*, 2017, **8**, 1708-1713.
49. S.-L. Suraru, J. A. Lee and C. K. Luscombe, *ACS Macro Lett.*, 2016, **5**, 533-536.
50. Y. Qiu, J. Mohin, C.-H. Tsai, S. Tristram-Nagle, R. R. Gil, T. Kowalewski and K. J. T. Noonan, *Macromol. Rapid Commun.*, 2015, **36**, 840-844.
51. Z. J. Bryan, M. L. Smith and A. J. McNeil, *Macromol. Rapid Commun.*, 2012, **33**, 842-847.
52. T. Hardeman and G. Koeckelberghs, *Polym. Chem.*, 2017, **8**, 3999-4004.
53. C. Valente, S. Çalimsiz, K. H. Hoi, D. Mallik, M. Sayah and M. G. Organ, *Angew. Chem. Int. Ed.*, 2012, **51**, 3314-3332.
54. A. K. Leone, P. K. Goldberg and A. J. McNeil, *J. Am. Chem. Soc.*, 2018, **140**, 7846-7850.
55. W. J. Marshall and V. V. Grushin, *Organometallics*, 2003, **22**, 1591-1593.
56. S. Caddick, F. G. N. Cloke, P. B. Hitchcock, J. Leonard, A. K. d. K. Lewis, D. McKerrecher and L. R. Titcomb, *Organometallics*, 2002, **21**, 4318-4319.
57. D. S. McGuinness, K. J. Cavell, B. W. Skelton and A. H. White, *Organometallics*, 1999, **18**, 1596-1605.
58. P. Kohn, S. Huettner, H. Komber, V. Senkovskyy, R. Tkachov, A. Kiriy, R. H. Friend, U. Steiner, W. T. S. Huck, J.-U. Sommer and M. Sommer, *J. Am. Chem. Soc.*, 2012, **134**, 4790-4805.
59. V. M. Chernyshev, O. V. Khazipov, M. A. Shevchenko, A. Y. Chernenko, A. V. Astakhov, D. B. Eremin, D. V. Pasyukov, A. S. Kashin and V. P. Ananikov, *Chem. Sci.*, 2018, **9**, 5564-5577.
60. A. V. Astakhov, O. V. Khazipov, E. S. Degtyareva, V. N. Khrustalev, V. M. Chernyshev and V. P. Ananikov, *Organometallics*, 2015, **34**, 5759-5766.
61. M. A. Baker, S. F. Zahn, A. J. Varni, C.-H. Tsai and K. J. T. Noonan, *Macromolecules*, 2018, **51**, 5911-5917.
62. A. Rudin, K. F. O'Driscoll and M. S. Rumack, *Polymer*, 1981, **22**, 740-747.
63. C. R. Bridges, C. Guo, H. Yan, M. B. Miltenburg, P. Li, Y. Li and D. S. Seferos, *Macromolecules*, 2015, **48**, 5587-5595.
64. J. Clark, J.-F. Chang, F. C. Spano, R. H. Friend and C. Silva, *Appl. Phys. Lett.*, 2009, **94**, 163306.
65. F. C. Spano, *Chem. Phys.*, 2006, **325**, 22-35.